The FASEB Journal article fj.201700002R. Published online May 1, 2017.



# PGLP-1, a novel long-acting dual-function GLP-1 analog, ameliorates streptozotocin-induced hyperglycemia and inhibits body weight loss

**Huashan Gao,*,† Qian Zhao,* Ziwei Song,* Zhaocong Yang,* You Wu,* Shanshan Tang,* Murad Alahdal,* Yanfeng Zhang,*,[1] and Liang Jin*,[1,2]**

*State Key Laboratory of Natural Medicines, Jiangsu Key Laboratory of Drug Screening, School of Life Science and Technology, China Pharmaceutical University, Nanjing, China; and †College of Chemistry and Chemical Engineering, Pingdingshan University, Pingdingshan, China

**ABSTRACT: It is well known that glucagon-like peptide 1 (GLP-1) has antidiabetic action. It has 2 distinct functions, an insulinotropic effect dependent on GLP-1 receptor (GLP-1R) and an insulinomimetic effect independent of GLP-1R. However, use of GLP-1 *in vivo* is limited by its short half-life. Therefore, our lab designed PGLP-1, a novel 2-function candidate peptide as a potential substitute. Using a streptozotocin-induced hyperglycemic mouse model, we demonstrated *in vitro* and *in vivo* that PGLP-1 had insulinotropic actions dependent on GLP-1R and insulinomimetic functions independent of GLP-1R. PGLP-1 treatment increased islet β-cell mass, plasma insulin, and C-peptide levels and Ki-67-immunoreactive β-cell numbers, verifying that PGLP-1 can work as a short GLP-1R agonist, similar to commercially available exendin-4. Additionally, PGLP-1 improved insulin sensitivity, inhibited gluconeogenesis by increasing expression of AMPK and receptor subfamily 0, group B, member 2 (SHP), and inhibited body weight loss by inhibiting β-oxidation, suggesting that PGLP-1 had insulinomimetic action. Taken together, these data indicated that PGLP-1, as a dual-function peptide, improved glycemic control and inhibited body weight loss, suggesting it could be useful for type 1 diabetes mellitus patients as an adjunctive therapy to insulin.—Gao, H., Zhao, Q., Song, Z., Yang, Z., Wu, Y., Tang, S., Alahdal, M., Zhang, Y., Jin, L. PGLP-1, a novel long-acting dual-function GLP-1 analog, ameliorates streptozotocin-induced hyperglycemia and inhibits body weight loss. FASEB J. 31, 000–000 (2017). www.fasebj.org**

**KEY WORDS: β-cell mass · β-oxidation · gluconeogenesis · insulinomimetic · insulinotropic**

Glucagon-like peptide 1 (GLP-1) is considered an incretin hormone that is secreted into the blood stream by intestinal L-cells in response to eaten food (1, 2). It stimulates insulin release, inhibits glucagon secretion, delays gastric emptying, and reduces appetite (3). GLP-1 can also increase β-cell mass by stimulating β-cell proliferation and inhibiting apoptosis (4, 5). Moreover, GLP-1(9-36)amide was defined as a product of GLP-1 (7-36)amide degradation by the dipeptidyl peptidase IV (DPP-IV). Because of its weak insulin-tropic activities, it was often referred to as the inactive metabolite of GLP-1. Recently, however, GLP-1(9-36)amide was suggested to have extrapancreatic insulin-like actions (insulinomimetic action) on insulin-sensitive tissues such as heart, vasculature, and liver (6, 7). Infusion of GLP-1(9-36)amide in obese insulin-resistant subjects was noted to acutely lower hepatic glucose production (8). GLP-1(9-36) amide was also demonstrated to inhibit glucose production by the inhibition of gluconeogenesis in isolated mouse hepatocytes *in vitro* (9), and *in vivo*, GLP-1(9-36) amide metabolite attenuated diabetes in diet-induced obese mice (10). Additionally, the nona-peptide GLP-1 (28-36)amide, cleaved by neutral endopeptidase NEP 24.11, improved β-cell mass in streptozotocin (STZ) induced diabetic mice (11).

**ABBREVIATIONS:** ACOX1, acyl-CoA oxidase 1; AUC, area under the concentration–time curve; CPT1A, carnitine palmitoyltransferase 1A; DPP-IV, dipeptidyl peptidase IV; G6Pase, glucose-6-phosphatase; GFP, green fluorescent protein; GLP-1, glucagon-like peptide 1; GLP-1R, glucagon-like peptide 1 receptor; GTT, glucose tolerance test; HEK-293, human embryonic kidney 293; ITT, insulin tolerance test; MD, molecular dynamic; PDB, Research Collaboratory for Structural Bioinformatics (RCSB) Protein Data Bank; PEPCK, phosphoenolpyruvate carboxykinase; PGLP, long-acting glucagon-like peptide 1 analog; PPAR, peroxisome proliferator-activated receptor; qPCR, quantitative PCR; QUICKI, Quantitative Insulin Sensititvity Index; SHP, receptor subfamily 0, group B, member 2; STZ, streptozotocin

[1] These authors contributed equally to this work.

[2] Correspondence. State Key Laboratory of Natural Medicines, Jiangsu Key Laboratory of Drug Screening, School of Life Science and Technology, China Pharmaceutical University, 24 Tongjia Alley, Gulou Qu, Nanjing Shi, Jiangsu Sheng, China, 210009. E-mail: liangjin1975@cpu.edu.cm

doi: 10.1096/fj.201700002R
This article includes supplemental data. Please visit *http://www.fasebj.org* to obtain this information.


 

Collectively, these reports indicate that GLP-1 has 2 distinct functions: a GLP-1-receptor (GLP-1R)-dependent insulinotropic function and a GLP-1R-independent insulinomimetic function that is mediated by GLP-1(9-36) amide. Natural GLP-1, however, has a short biologic half-life of 2 to 3 min (12), thus limiting its therapeutic potential. While synthetic substitutes with a longer half-life, such as exendin-4 and liraglutide, have successfully mimicked the insulinotropic effects of GLP-1, they have lost insulinomimetic function caused by GLP-1(9-36)amide. The aim of our lab was to design a GLP-1 analog with an improved half-life that can function as a GLP-1R agonist and that can break down into GLP-1(9-36) for insulinomimetic actions. Here we demonstrate that our long-acting GLP-1 analog, PGLP-1, has both insulinotropic and insulinomimetic function.

## MATERIALS AND METHODS

### Peptide synthesis

Exendin-4, GLP-1, PEP-1, PEP-2, PEP-3, PEP-4, PEP-5, GLP-1(9-37), PGLP-1(9-38), and PGLP-1 were chemically synthesized by GL Biochem (Shanghai, China).

### Homology model

The crystal structure of GLP-1/GLP-1R was downloaded from the Research Collaboratory for Structural Bioinformatics (RCSB) Protein Data Bank (PDB) (*http://www.rcsb.org/pdb/home/home.do;* No. 3IOL). The active form of GLP-1 is GLP-1(7-37), whereas the structure of GLP-1 on PDB Web site lacks $His^{7}$, $Ala^{8}$, $Glu^{9}$, $Arg^{36}$, and $Gly^{37}$ (13). Homologous modeling was performed by using MOE2009 to complement the residues. Then 100 ns molecular dynamic (MD) simulation was performed by using the scoring function. The structure of the top 3 was selected for binding energy analysis. Optimal configuration was wild-type GLP-1, and the mutant peptides (PEP-1, PEP-2, PEP-3, PEP-4, PEP-5 and PGLP-1) were designed with the mutant configuration.

### MD simulations

MD modeling of GLP-1/GLP-1R and mutant peptides/GLP-1R was performed by AMBER 12. The system uses the ff14SB force field. In order to simulate the solvent environment, a periodic box of TIP3P water molecules that extends to 8.0 Å from the protein atoms was added into the model (14, 15). In addition, $Na^{+}$ was added as a counter ion to maintain an electrically neutral receptor–ligand system.

First, the energy optimization of the entire system was performed using the steepest descent minimization of 5000 steps and the conjugate gradient minimization of 5000 steps. In the process of energy optimization, the cutoff value of the nonkey interaction was set to 10.0 Å, the constant volume periodic boundary was used, and the long-range electrostatic energy was calculated using the particle-mesh Ewald method. Then the heating of each system was conducted within 500 ps from 0.0 K to 300.0 K at 2.0 kcal · $mol^{-1}$ Å-2 positional restraints on protein. Next each system was equilibrated for 5 ns under a NPT ensemble at a constant temperature of 300 K and a constant pressure of 1.0 bar.

Afterward, the production MD simulations were performed for 100 ns for each system. Because the receptor structure was incomplete, the PDB structure contains only the extracellular domain, so the binding at $Thr^{2}$, $Val^{3}$, $Glu^{100}$, $Glu^{101}$, $Thr^{107}$, $Phe^{108}$, $Thr^{109}$, and $Ser^{110}$ residues at 1.00 kcal · $mol^{-1}$. The SHAKE algorithm was used to constrain bonds involving hydrogen atoms, and the time step was set to 2 fs. The data were collected every 10 ps for further analysis. Simulations of each complex were repeated 3 times based on our existing calculation conditions.

### Cell line and cell culture

Human embryonic kidney 293 (HEK-293) cells and MIN6 cells were obtained from American Type Culture Collection (ATCC, Manassas, VA, USA) and confirmed to be mycoplasma free. HEK-293 cells were cultured in DMEM containing 25 mM glucose supplemented with 10% fetal bovine serum, 100 μg/ml penicillin and 100 μg/ml streptomycin at 37°C, and 5% $CO_2$ in a humidified incubator. The cell culture media and reagents were obtained from Thermo Fisher Scientific (Waltham, MA, USA). MIN6 cells were cultured in DMEM supplemented with 10% heat-inactivated fetal bovine serum, 1 mM L-glutamine, 100 μg/ml penicillin, 100 μg/ml streptomycin, and 55 μM β-mercaptoethanol at 37°C and 5% $CO_2$ in a humidified incubator.

### Human GLP-1 receptor activation

GLP-1 or GLP-1 analogs were tested for their ability to activate the GLP-1 receptor (GLP-1R) using a cell-based green fluorescent protein (GFP) reporter gene assay that indirectly measures cAMP induction. HEK-293 cells were cotransfected with the plasmid pcDNA3.1(+)-HuGLP-1R (geneticin selection) containing human GLP-1R cDNA and the plasmid PGL4.22-6×CRE-vip-GFP (puromycin selection) with a GFP reporter gene construct fused to 6 continuous cAMP response elements (CRE) and a micro promoter (vip) (16). The cotransfected HEK-293 cells were seeded on 24-well plates (Corning, Corning, NY, USA) at a density of 80,000 cells per well, then incubated for 12 h at 37°C and 5% $CO_2$ in a humidified environment. Then serial dilutions of GLP-1 or GLP-1 analogs with serum-free culture medium were added to the wells (500 μl per well). After incubation at 37°C and 5% $CO_2$ in a humidified environment for 8 h, the cells were manipulated into a single cell suspension with trypsin-EDTA solution and analyzed by Flowcytometer (BD Accuri, C6; BD Biosciences, San Jose, CA, USA). The proportion of GFP-expressing cell was analyzed using BD Accuri C6 1.0.264.21 software. The data were graphed against concentration of peptide, and EC50 values were calculated by GraphPad Prism 5.0 software (GraphPad Software, La Jolla, CA, USA). Activation of the GLP-1 receptor was further measured by assessing the cAMP formation in MIN6 cells. MIN6 cells were cultured and seeded onto 96-well plates as described above. Then serial dilutions of peptides were added separately and incubated for 15 min. The cells were collected for cAMP detection. cAMP content was determined with the cAMP Parameter Assay Kit (R&D Systems, Minneapolis, MN, USA).

### Stability test for DPP-IV *in vitro*

GLP-1 or GLP-1 analogs (20 μM) were incubated at 37°C with isopyknic 0.2 ng/μl rhDPP-IV (R&D Systems) for various durations in 25 mM Tris, pH 8.0 (final peptide concentration 10 μM). Enzymatic reactions were terminated by the addition of 5 μl of 10% (v/v) trifluoroacetic acid/water and stored at −20°C before HPLC analysis. The concentration of treated samples was determined by a reverse-phase HPLC system at room temperature with a C18 chromatographic column (150 × 4.6 mm × 5 μm; Shimadzu, Tokyo, Japan). The chromatography was performed with a linear gradient elution from 20% to 85% acetonitrile in ultrapure water

containing 0.05% trifluoroacetic acid for 12 min. The flow rate was 1 ml/min, and the UV absorbance was set at 215 nm.

### Intraperitoneal glucose tolerance test and insulin tolerance test

An intraperitoneal glucose tolerance test (GTT) was performed with 1.5 g/kg glucose in normal C57BL/6J mice (7–8 wk old). Intraperitoneal GTTs and insulin tolerance tests (ITTs) were performed with 1 g/kg glucose or 0.5 U/kg insulin into STZ-induced hyperglycemic C57BL/6J mice, respectively. Quantitative Insulin Sensitivity Check Index (QUICKI) values were calculated by the following formula: [1/(log (fasting insulin μU/ml) + log (fasting glucose mg/dl)].

### Mice and STZ *in vivo* treatment

C57BL/6J mice (7–8 wk old) were obtained from Model Animal Research Center of Nanjing University (Nanjing, China). Mice were housed singly or in groups on a 12 h/12 h light–dark cycle at 22°C with free access to food and water.

Male C57BL/6J mice were injected intraperitoneally with STZ (50 mg/kg body weight ; Sigma-Aldrich, St. Louis, MO, USA) dissolved in saline or 200 μl of saline (vehicle) for 5 consecutive days, starting on d 0 (17, 18). Blood glucose concentrations were measured at 7 and 14 d after the last injection of STZ with a blood glucose meter (Omron, Tokyo, Japan). Blood samples were obtained from the tail vein of unfed mice. Mice with 2 blood glucose measurements above 11.1 mM were considered hyperglycemic. All animals were fed according to the protocols of the National Institutes of Health (Bethesda, MD, USA) and granted by the China Pharmaceutical University Institute Animal Care and Use Committee (Nanjing, China).

### Gluconeogenesis detection

Hyperglycemic C57BL/6J mice were divided into 5 groups as vehicle, GLP-1(9-37), PGLP-1(9-38), GLP-1, and PGLP-1. Every group was injected subcutaneously with placebo or 30 nmol/kg of peptides, respectively. The mice were humanely killed by isoflurane overdose 1 h after injection, and the dissected tissues were immediately frozen in liquid nitrogen unless otherwise stated.

### Chronic *in vivo* studies

Hyperglycemic C57BL/6J mice were divided into 4 groups: vehicle, GLP-1, PGLP-1, and exendin-4. Every group was subcutaneously injected twice daily with placebo or 30 nmol/kg of peptides for 5 wk. Fasting blood glucose (unfed 8 h) and body weight were assayed weekly, and food intake was measured every 2 or 3 d. Animals were humanely killed by isoflurane overdose, and dissected tissues were immediately frozen in liquid nitrogen, unless otherwise stated. Blood samples were collected from the eye socket and centrifuged, and then serum was collected. Serum insulin, glucagon, and C-peptide levels were measured by ELISA kits (Nanjing JianCheng Institute, Nanjing, China).

### Histologic examination

Pancreata were fixed in 4% paraformaldehyde overnight at 4°C and embedded in paraffin blocks. Sections (7 μm thick) were stained with hematoxylin and eosin. Deparaffinized and rehydrated sections were permeabilized in 0.2% Triton X-100 for 5 min and blocked in PBST containing 10% bovine serum albumin for 90 min. Primary antibodies were diluted in the same solution, applied onto sections, and incubated overnight at 4°C. Slides were washed in PBST and incubated for 60 min with the appropriate secondary antibody. Slides were washed in PBS, mounted with DAPI, and viewed by fluorescence microscopy (19). Rabbit anti-mouse Ki-67 (dilution 1: 200; Abcam, Cambridge, MA, USA) and guinea pig anti-mouse insulin (dilution 1: 300; Abcam) were used as the primary antibody. The secondary antibodies used for immunofluorescence were donkey anti-rabbit IgG H&L (Alexa Fluor 647) and goat anti–guinea pig IgG H&L (Alexa Fluor 488).

The sections were examined with an Olympus microscope (Olympus, Tokyo, Japan) and systematically scanned with a computer with imaging software to control the data collection. The percentage of β-cell area per whole pancreas was then calculated. Cell mass was calculated by β-cell area multiplied by whole pancreas weight (20).

### Real-time quantitative PCR

Mouse livers were pulverized in liquid nitrogen, and total RNA was prepared using Trizol (Thermo Fisher Scientific). cDNA was prepared by HiScript Q RT SuperMix for quantitative PCR (qPCR) (Vazyme, Nanjing, China), and real-time PCR assays were carried out with a LC480 Light Cycler (Roche, Basel, Switzerland) using the applied primer sequences listed in Supplemental Table 3.

### Western blot analysis

Liver tissues were lysed in lysis buffer. After addition of loading buffer, boiling samples were boiled and separated by 10% or 12% SDS-PAGE. Proteins were transferred to PVDF membranes, and unspecific binding sites were blocked with Western blot blocking solution (Beyotime Institute of Biotechnology, Nanjing, China). The following primary antibodies were used: anti-phosphoenolpyruvate carboxykinase (PEPCK), anti-glucose-6-phosphatase (G6Pase), anti-AMPK (Thr 172, phosphorylated at threonine 172), anti–nuclear receptor subfamily 0, group B, member 2 (SHP, or NR0B2), anti-carnitine palmitoyltransferase 1A (CPT1A), anti-acyl-CoA oxidase 1 (ACOX1), anti–peroxisome proliferator-activated receptor (PPAR) β/δ, and anti-GAPDH. For quantification of optical density, TanonImage 1.00 software (Tanon, Shanghai, China) was used.

### Statistical analysis

Data were expressed as means ± SEM and analyzed by SPSS 13.0 for Windows (IBM SPSS, Chicago, IL, USA). Statistical significance was determined by Student's *t* test or 1-way ANOVA followed by the Student-Newman-Keuls *post hoc* test. Differences were considered statistically significant at $P < 0.05$.

## RESULTS

### Design of sequence and receptor–ligand binding prediction

To obtain a dual-function analog, we designed 6 peptides (Supplemental Fig. 1*A* and **Fig. 1*A***). First we used MD simulation to explore whether the binding between ligand and receptor changed. The MD simulations were

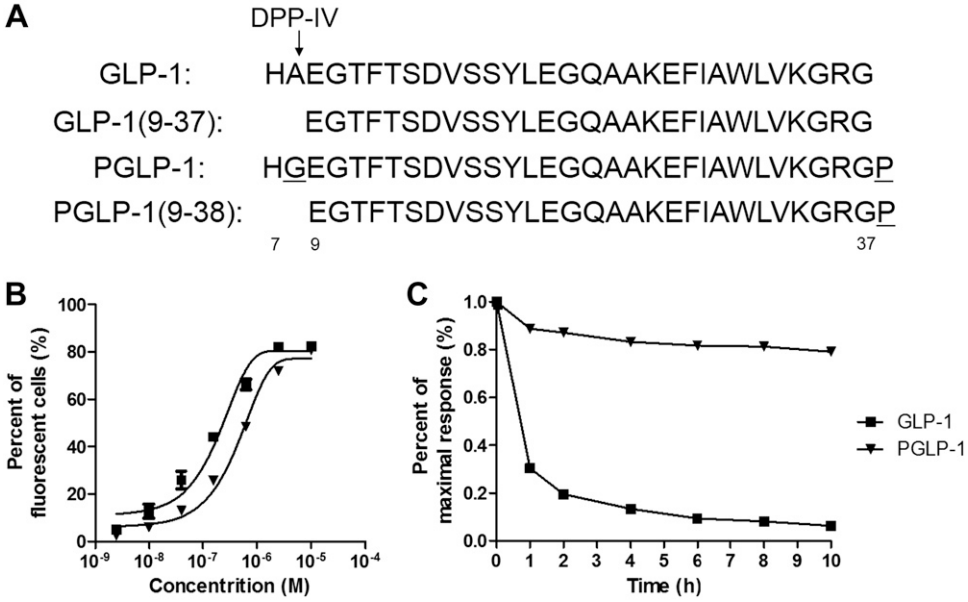


**Figure 1.** Biologic activity of PGLP-1. *A*) Sequences of native GLP-1, GLP-1(9-37), PGLP-1, and PGLP-1(9-38). *B*) Representative dose–response curves for activation of human GLP-1R by native GLP-1 or PGLP-1. *C*) Stability of PGLP-1 and native GLP-1 against enzymatic degradation by DPP-IV.

performed for 100 ns for each system. In addition, the molecular mechanics Poisson-Boltzmann surface area binding energy of the complex was calculated (Supplemental Fig. 1*B–H* and Supplemental Table 1). The binding energies were stable from 10 ns to the end of the simulation. The smaller the final binding energy at the end of the MD, the better the affinity between receptor and ligand. As seen in Supplemental Table 1, the best binding condition was the wild type ($-54.73$ kcal $\cdot$ mol$^{-1}$), which was followed by the mutant peptide PGLP-1 ($-43.44$ kcal $\cdot$ mol$^{-1}$). Other mutant peptides had higher binding energy, indicating that the altered residues had a large effect on receptor–ligand binding. These data suggested that PGLP-1 might be a candidate peptide.

## Bioactivity and stability analysis of PGLP-1 *in vitro*

Subsequently, the analogs were tested for receptor–ligand binding activity *in vitro*. Consistent with the receptor–ligand binding prediction results, receptor activity of all analogs were reduced by different degrees. PEP-1, -2, and -3 did not activate the GLP-1R (Supplemental Fig. 2*A*). PEP-4 and -5 had decreased affinity (Supplemental Fig. 2*A*). PGLP-1 (Fig. 1*B*) could activate GLP-1R in a dose-dependent manner, and the EC50 was only slightly increased (GLP-1 was 150 $\pm$ 40.2 nM and PGLP-1 369 $\pm$ 133 nM; no significant difference). In a mouse pancreatic β-cell line (MIN6) that abundantly expresses GLP-1R, cAMP production induced by PGLP-1 was also slightly increased compared to GLP-1 (Supplemental Table 2). To evaluate the stability of PGLP-1 against degradation by DPP-IV *in vitro*, HPLC was used (21). All peptides were incubated with the DPP-IV enzyme at 37°C for 1 to 10 h and the proportion of remaining intact peptides assessed. After incubation for 1 h, 34.7% of intact GLP-1 remained, whereas after incubating for 10 h, only 6.3% of intact GLP-1 had remained. PEP-4 and -5 partially resisted degradation by DPP-IV (Supplemental Fig. 2*B*), whereas PGLP-1 almost completely resisted degradation by DPP-IV, with over 80% of intact PGLP-1 remaining after 10 h of incubation (Fig. 1*C*).

## Acute and sustained hypoglycemic effect of PGLP-1 in normal C57BL/6J mice

To investigate whether the analogs possessed GLP-1R activity *in vivo*, we compared their acute glycemic effects in normal C57BL/6J mice. PEP-1, -2, -3, and -4 had negligible hypoglycemic effect (Supplemental Fig. 3*A, B*), PEP-5 had some hypoglycemic effect (Supplemental Fig. 3*A, B*), and PGLP-1 (**Fig. 2*A***) had comparable hypoglycemic effect as GLP-1 *in vivo*. Furthermore, subcutaneous injection of PGLP-1 at 1, 30, or 100 nmol/kg demonstrated dose-dependent hypoglycemic effect *in vivo* compared to GLP-1 (30 nmol/kg) (Fig. 2*A*). This verified that PGLP-1 had acute insulinotropic activity.

To evaluate the sustained hypoglycemic effect, a single dose of PGLP-1 (30 nmol/kg), GLP-1 (30 nmol/kg), or placebo was subcutaneously administrated. As shown in Fig. 2*B*, the hypoglycemic effect of PGLP-1 was still evident at 2 h after administration, and the trend continued to 4 h. In contrast, the hypoglycemic effect of native GLP-1 lasted less than 1 h, confirming that PGLP-1 could work as a sustained GLP-1R agonist.

## Acute inhibition of gluconeogenesis gene expression by PGLP-1

To prove whether PGLP-1 and PGLP-1(9-38) have the same gluconeogenesis inhibition as GLP-1, hyperglycemic STZ-induced mice were subcutaneously injected once with the above-mentioned peptides, and the liver was removed 1 h after injection for qPCR and Western blot

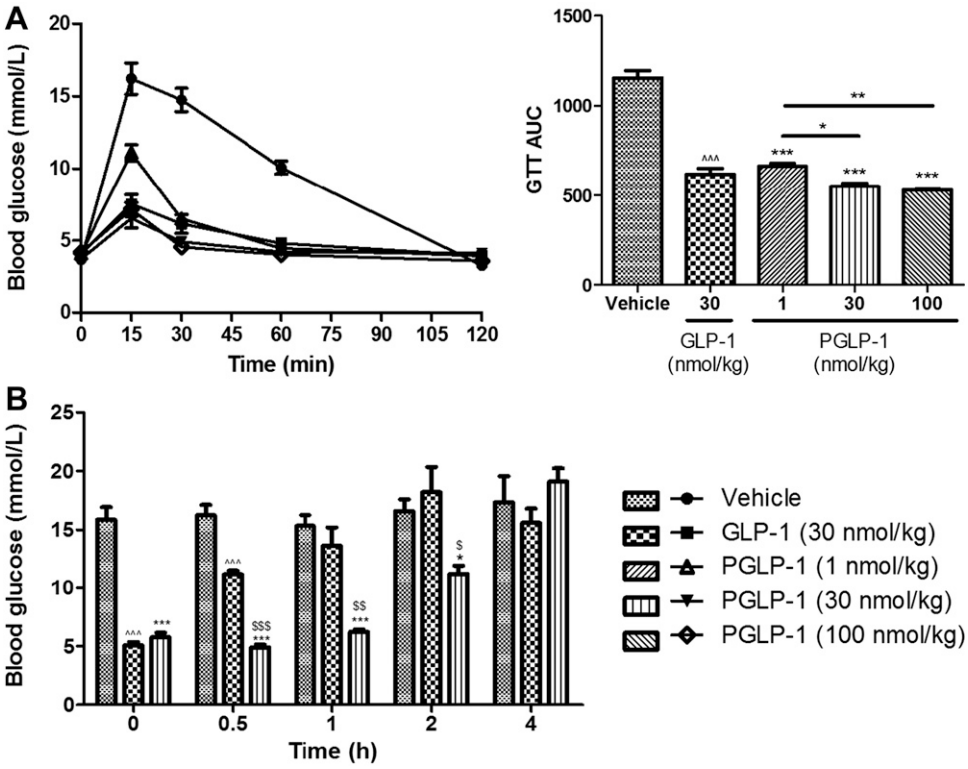


**Figure 2.** Acute effects on intraperitoneal GTT in unfed male C57BL/6J mice (age 8 wk; $n = 6$ mice per group) after single injection. *A*) Blood glucose levels after single injection of placebo, GLP-1 (30 nmol/kg), or PGLP-1 (1, 30, 100 nmol/kg). *B*) Blood glucose levels (during intraperitoneal GTT, time = 15 min) at different times after subcutaneous administration of placebo, GLP-1 (30 nmol/kg) or PGLP-1 (30 nmol/kg). $^{*}P < 0.05$; $^{***}P < 0.001$, PGLP-1 compared to vehicle group; $^{\wedge\wedge\wedge}P < 0.001$, GLP-1 compared to vehicle group; $^{\$}P < 0.001$; $^{\$\$}P < 0.001$; $^{\$\$\$}P < 0.001$, PGLP-1 compared to GLP-1 group.

analyses. The results revealed that GLP-1(9-37), PGLP-1(9-38), GLP-1, and PGLP-1 could all significantly reduce the mRNA levels of both PEPCK and G6Pase compared to vehicle (PGLP-1, PGLP-1(9-38), $P < 0.001$; and GLP-1, GLP-1(9-37), $P < 0.01$) (**Fig. 3*A, B***). Likewise, protein expression for both PEPCK and G6Pase was reduced by ~50% in mice receiving GLP-1(9-37), PGLP-1(9-38), GLP-1, and PGLP-1 (Fig. 3*C, D*). There was no significant difference between GLP-1(9-37) and PGLP-1(9-38).

## PGLP-1 ameliorates STZ-induced hyperglycemia by increasing insulin level and improving insulin sensitivity

Beginning with wk 2, fasting blood glucose of PGLP-1-treated mice was significantly decreased compared to vehicle group (**Fig. 4*A***), and at wk 5, fasting blood glucose dropped to 9.6 mM (compared to vehicle group, $P < 0.05$). The positive controls GLP-1 and exendin-4 only had a partial decrease in blood glucose (GLP-1 12.2 mM; exendin-4 11.9 mM; no significant difference compared to vehicle). PGLP-1 treatment also significantly increased insulin levels (Fig. 4*B*), whereas GLP-1 and exendin-4 did not. In addition, PGLP-1 treatment increased the C-peptide level, which was significantly different compared to exendin-4 (Fig. 4*C*).

QUICKI, a well-established marker for insulin sensitivity, was increased in PGLP-1 group (Fig. 4*D*). These findings suggested that PGLP-1 treatment may improve systemic insulin sensitivity; therefore, we next determined glucose and insulin tolerance. PGLP-1 treatment significantly improved glucose and insulin tolerance in STZ-induced hyperglycemic mice (Fig. 4*E–H*). GTT area under the concentration–time curve (AUC) showed that PGLP-1 had smaller AUC than exendin-4 compared to vehicle group (PGLP-1, $P < 0.01$; exendin-4, $P < 0.05$) (Fig. 4*F*). PGLP-1 had smaller ITT AUC than exendin-4 compared to vehicle group (PGLP-1 $P < 0.05$; exendin-4, NS) (Fig. 4*H*). Meanwhile, PGLP-1 treatment reduced glucagon levels (Fig. 4*I*).

## PGLP-1 inhibited body weight loss and improved energy utilization

STZ-induced hyperglycemic mice were treated with vehicle PGLP-1, GLP-1, or exendin-4 for a period of 5 wk. Body weight loss was significant among all experimental groups except for mice treated with PGLP-1 (**Fig. 5*A, B***). Even at wk 1, PGLP-1 mice showed minimal weight loss compared to the drastic weight loss in other groups. By wk 4 and 5, PGLP-1 significantly increased body weight compared to vehicle group ($P < 0.05$). To further understand the difference in weight gain, cumulative energy intake was evaluated. STZ-induced hyperglycemic mice treated with PGLP-1 and exendin-4 displayed a significantly lower cumulative energy intake from wk 2 (Fig. 5*C*). At wk 5, PGLP-1 treatment was more anorectic when energy intake was normalized to body weight (Fig. 5*D*).

## PGLP-1 increases β-cell mass and promotes β-cell proliferation

Because pancreatic endocrine β cells play a central role in glucose metabolism, pancreata were taken from STZ mice and analyzed by hematoxylin and eosin staining. The

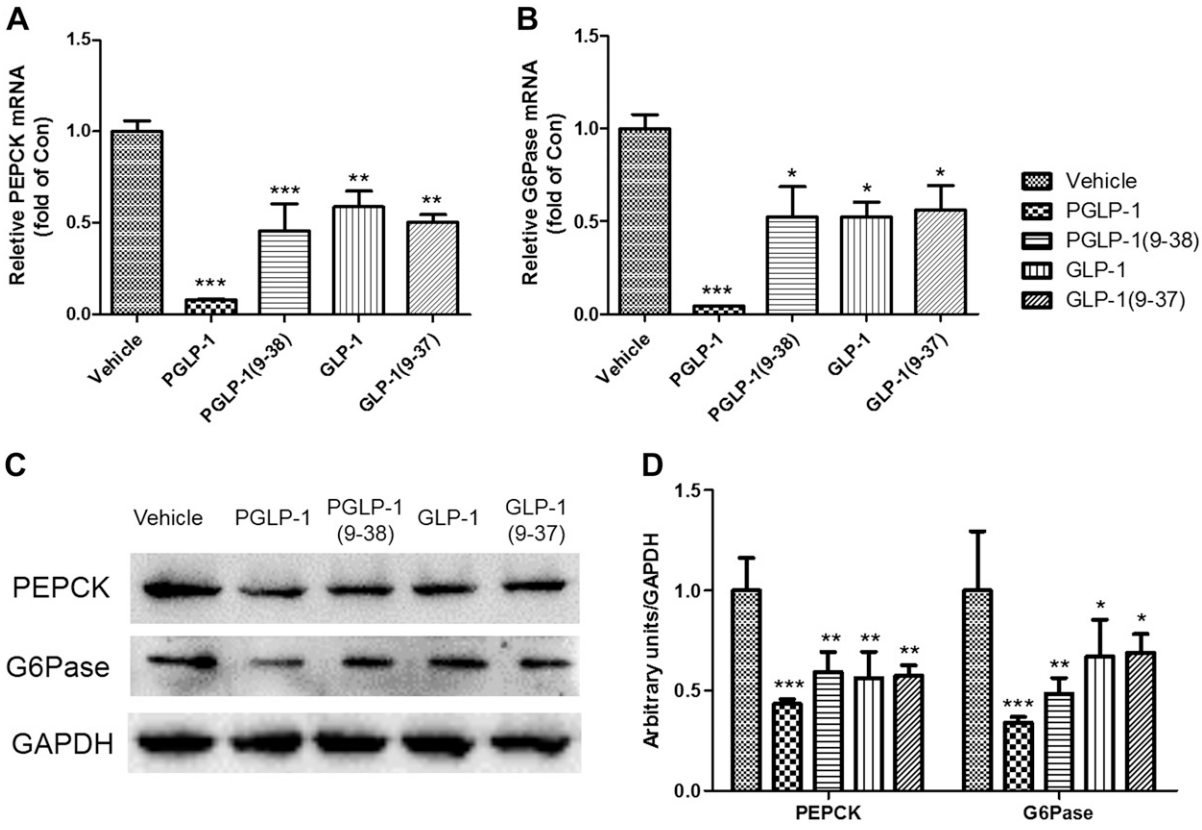


**Figure 3.** Acute effects of single injection of GLP-1, PGLP-1, GLP-1(9-37), and PGLP-1(9-38) on expression of genes associated with gluconeogenesis. *A–B*) Expression of PEPCK (*A*) and G6Pase (*B*) mRNA levels ($n = 6$ mice per group). *C*) Western blot analysis of PEPCK and G6pase protein in the liver. *D*) Quantification of Western blot ($n = 3$ mice per group).

results revealed that islet structure was severely damaged in the vehicle group. In the GLP-1, exendin-4, and PGLP-1 groups, however, the damage was limited and islet structure remained intact (**Fig. 6*A***). Thus, GLP-1, exendin-4, or PGLP-1 treatment exhibited a protective effect on islet morphology. To further assess whether pancreatic endocrine β-cell mass increased, insulin and Ki-67 double immunofluorescence staining was performed. GLP-1, exendin-4, and PGLP-1 treatment significantly increased β-cell mass (Fig. 6*B*). Compared to vehicle, GLP-1 and exendin-4 increased β-cell mass by 2-fold, and PGLP-1 resulted in about a 4-fold increase (Fig. 6*C*). The islet numbers did not increase in any of groups (Fig. 6*D*). Because GLP-1 agonist can increase β-cell mass by stimulating β-cell proliferation (5), we determined Ki-67-immunoreactive β-cells. Ki-67-immunoreactive β cells were also similarly increased in the exendin-4 and PGLP-1 groups, whereas the GLP-1 group was not increased compared to the vehicle group (Fig. 6*B*, *E*).

## PGLP-1 reduces mRNA and protein levels of gluconeogenesis genes by increasing AMPK and SHP protein levels in the liver

Because infusion of GLP-1(9-36)amide remarkably lowered hepatic glucose production (8), we examined the liver for effects of PGLP-1 on the expression of gluconeogenesis genes. The mRNA levels of both PEPCK and G6Pase in the liver were significantly reduced in mice treated with PGLP-1 compared to vehicle (**Fig. 7*A*, *B***). Likewise, protein expression for both PEPCK and G6Pase was reduced by ~30–60% in mice treated with PGLP-1 or exendin-4 (Fig. 7*D*, *E*). In addition, PGLP-1 treatment reduced protein expression levels of PEPCK and G6Pase to a greater extent compared to exendin-4. Transcriptional regulator SHP (also known as NR0B2), which is known to modulate hepatic gluconeogenesis, was increased in the livers of mice treated with PGLP-1 (Fig. 7*C*). Likewise, protein expression of SHP was significantly increased compared to vehicle group (Fig. 7*F*, *G*). Because the activation of AMPK transcriptionally enhances expression of SHP in the liver, we examined the activation of AMPK, which increased about 2-fold in the livers of mice receiving PGLP-1 (Fig. 7*F*, *G*). Although exendin-4 also increased SHP and AMPK protein levels, PGLP-1 treatment increased the protein expression levels of SHP and AMPK to a greater extent than exendin-4 (SHP, $P < 0.01$; AMPK, $P < 0.05$). The mRNA levels of other transcriptional regulators, such as PPAR-γ, peroxisome proliferative activated receptor γ coactivator 1 α (PGC1-α), forkhead box O1 (FOXO1), sterol regulatory element binding transcription factor 1 (SREBP1C), transcription factor 7–like 2, T-cell-specific, HMG box (TCF7L2), and nu clear receptor subfamily 0, group B, member 1 (DAX-1),

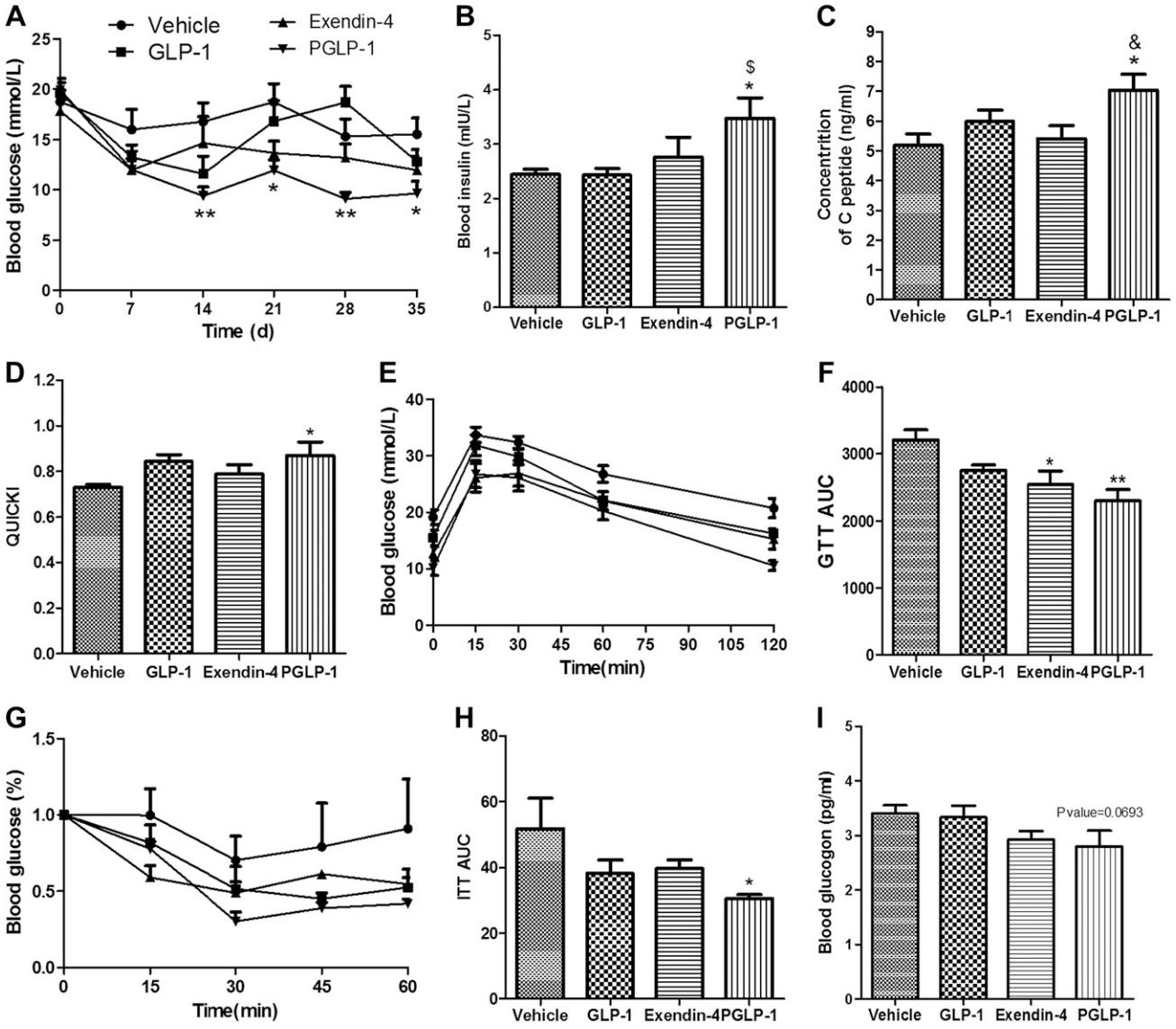


**Figure 4.** Chronic effect of GLP-1, PGLP-1, and exendin-4 on blood glucose over period of 5 wk. Subcutaneous treatment with GLP-1 (2 × 30 nmol/kg/d), exendin-4 (2 × 30 nmol/kg/d), PGLP-1 (2 × 30 nmol/kg/d), or placebo in STZ-induced hyperglycemic mice. *A–C*) Weekly measurements of fasted blood glucose (*A*), plasma insulin level (*B*), C-peptide level (*C*), and QUICKI (*D*). *E, F*) At wk 5 GTT and AUC evaluation. *G–H*) ITT normalized for basal blood glucose and AUC evaluation. *I*) Plasma glucagon level. $^{*}P < 0.05$; $^{**}P < 0.001$, PGLP-1 compared to vehicle group; $^{\$}P < 0.05$, PGLP-1 compared to GLP-1 group; $^{\&}P < 0.05$, PGLP-1 compared to exendin-4 group.

were not affected by PGLP-1 treatment (Supplemental Fig. 4*A–F*).

## PGLP-1 reduces mRNA and protein levels of β-oxidation genes in the liver

Unlike type 2 diabetes, in which obesity is a definitive risk factor and the significance of nonalcoholic steatohepatitis has been highlighted (22), there is some evidence that intrahepatic fat content is reduced in type 1 diabetes (23). This was associated with increased fasting lipid oxidation. Therefore, we examined β-oxidation levels in the liver of STZ-treated mice. The mRNA and protein expression levels of both CPT1A and ACOX1 in the liver were significantly reduced in PGLP-1-treated mice compared to the vehicle group (**Fig. 8*A, B, E, F***), and their mRNA and protein levels were significantly decreased compared to exendin-4-treated mice (CPT1A, $P < 0.05$; ACOX1, $P < 0.05$). PPAR-β, which is associated with fat oxidation (24), was also significantly reduced in the livers of PGLP-1-treated mice (Fig. 8*C*). UCP-2 mRNA level were also significantly reduced (Fig. 8*D*).

## DISCUSSION

GLP-1 possesses a number of antidiabetic actions, including glucose-dependent insulin secretion (insulinotropic action) (2) and insulin-like (insulinomimetic)

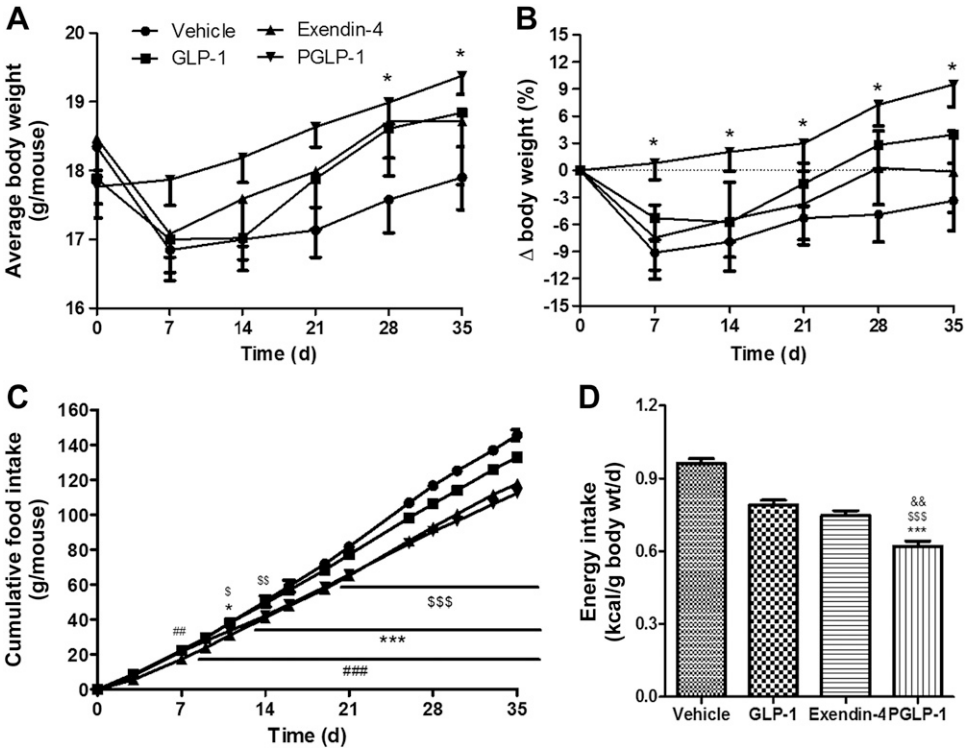


**Figure 5.** Body weight and energy intake in STZ-induced hyperglycemic mice. Weekly unfed body weight (*A*) change in body weight (*B*), and cumulative energy intake (*C*) during subcutaneous injection of GLP-1 (30 nmol/kg), PGLP-1 (30 nmol/kg), exendin-4 (30 nmol/kg), or placebo twice daily for 5 wk. *D*) Wk 5, after overnight food withdrawal (16–18 h), mice were placed in individual cages, and food intake was monitored over 24 h ($n$ = 3–4 per group). Data are expressed as kcal consumed per gram of body weight per day. $^{\#}P < 0.05$; $^{\#\#\#}P < 0.001$, exendin-4 compared to vehicle group; $^{*}P < 0.05$; $^{***}P < 0.001$, PGLP-1 compared to vehicle group; $^{\$}P < 0.001$; $^{\$\$}P < 0.001$; $^{\$\$\$}P < 0.001$, PGLP-1 compared to GLP-1 group; $^{\&}P < 0.001$; $^{\&\&}P < 0.001$; $^{\&\&\&}P < 0.001$, PGLP-1 compared to exendin-4 group.

action (9, 10, 25, 26) besides its insulinotropic action. However, GLP-1 has a half-life of only 2 to 3 min (12), thus limiting its therapeutic potential. This inspired us to design a long-acting dual-function GLP-1 analog. The goal was to improve half-life and generate an analog that can function as a GLP-1R agonist as well as break down into GLP-1(9-36)amide for insulinomimetic actions. The breakthrough was to add a Pro at the end of the GLP-1, to produce a partially DPP-IV-resistant analog PGLP-1. We demonstrate here that PGLP-1 has a similar affinity to GLP-1R *in vitro* and equivalent insulinotropic actions *in vivo* compared to native GLP-1. *In vitro,* HPLC result reveals that PGLP-1 can not only resist DPP-IV digestion but can also produce GLP-1(9-36)amide. This is verified by intraperitoneal GTT; a single injected dose of PGLP-1 can reduce blood glucose levels for over 2 h. However, the stability of PGLP-1 *in vitro* is shorter than *in vivo* because *in vivo,* the clearance of PGLP-1 is complex. Not only can PGLP-1 be degraded by enzymes (DPP-IV, neutral endopeptidase, etc.), but it can also easily be filtered out from the kidney. These data verified that PGLP-1 could effectively work as a GLP-1R agonist and meanwhile had a potential insulinomimetic PGLP-1(9-38). Because PGLP-1 (9-38) has a Pro at the end of the GLP-1(9-37), we determined the acute effects of PGLP-1(9-38) and GLP-1 (9-37) on the expression of genes associated with gluconeogenesis, and the results revealed that PGLP-1(9-38) and GLP-1(9-37) had the same inhibitory effect on gluconeogenesis.

To further confirm that PGLP-1 has both insulinotropic and insulinomimetic actions, we utilized an STZ-induced hyperglycemic mice model. The model was chosen because the insulin shortage allowed for the study of insulinomimetic action, while the small amount of remaining β cells allowed for the study of insulinotropic function. After 5 wk of treatment, PGLP-1 significantly ameliorated hyperglycemia and was more effective than either GLP-1 or exendin-4 (Fig. 4*A*). Furthermore, PGLP-1 treatment increased insulin and C-peptide secretion more than either GLP-1 or exendin-4 (Fig. 4*B, C*). This result suggests that PGLP-1 can work as a dual-function GLP-1 analog, given that exendin-4 is only a GLP-1R agonist and GLP-1 has a short half-life (12). Hematoxylin and eosin staining revealed that PGLP-1, GLP-1, and exendin-4 treatment preserved islet architecture compared to vehicle. Islet immunostaining revealed that GLP-1, exendin-4, and PGLP-1 treatment significantly increased β-cell mass compared to vehicle. Additionally, we noted that both PGLP-1 and exendin-4 treatment increased Ki-67-immunoreactive β-cell mass. This is consistent with the report that GLP-1R agonist can increase β-cell mass by stimulating β-cell proliferation (5), and it verifies that PGLP-1, as a GLP-1R agonist, can increase β-cell mass through stimulating β-cell proliferation dependent on GLP-1R. However, it does not explain why PGLP-1 treatment increased β-cell mass more than other groups. The islet number was examined, but it did not increase (Fig. 6*D*) in any treatment groups compared to vehicle. It is reported that GLP-1(28-36)amide protects pancreatic β-cell from glucolipotoxicity (27), and GLP-1 and PGLP-1 include GLP-1(28-36)amide, cleaved by neutral endopeptidase NEP 24.11. This suggested that GLP-1 and PGLP-1 increased β-cell mass through protection of GLP-1(28-36)amide independent of GLP-1R *in vivo.* All these data indicated that PGLP-1 increased β-cell mass through proliferation dependent on GLP-1R and protection of GLP-1(28-36)amide independent of GLP-1R.

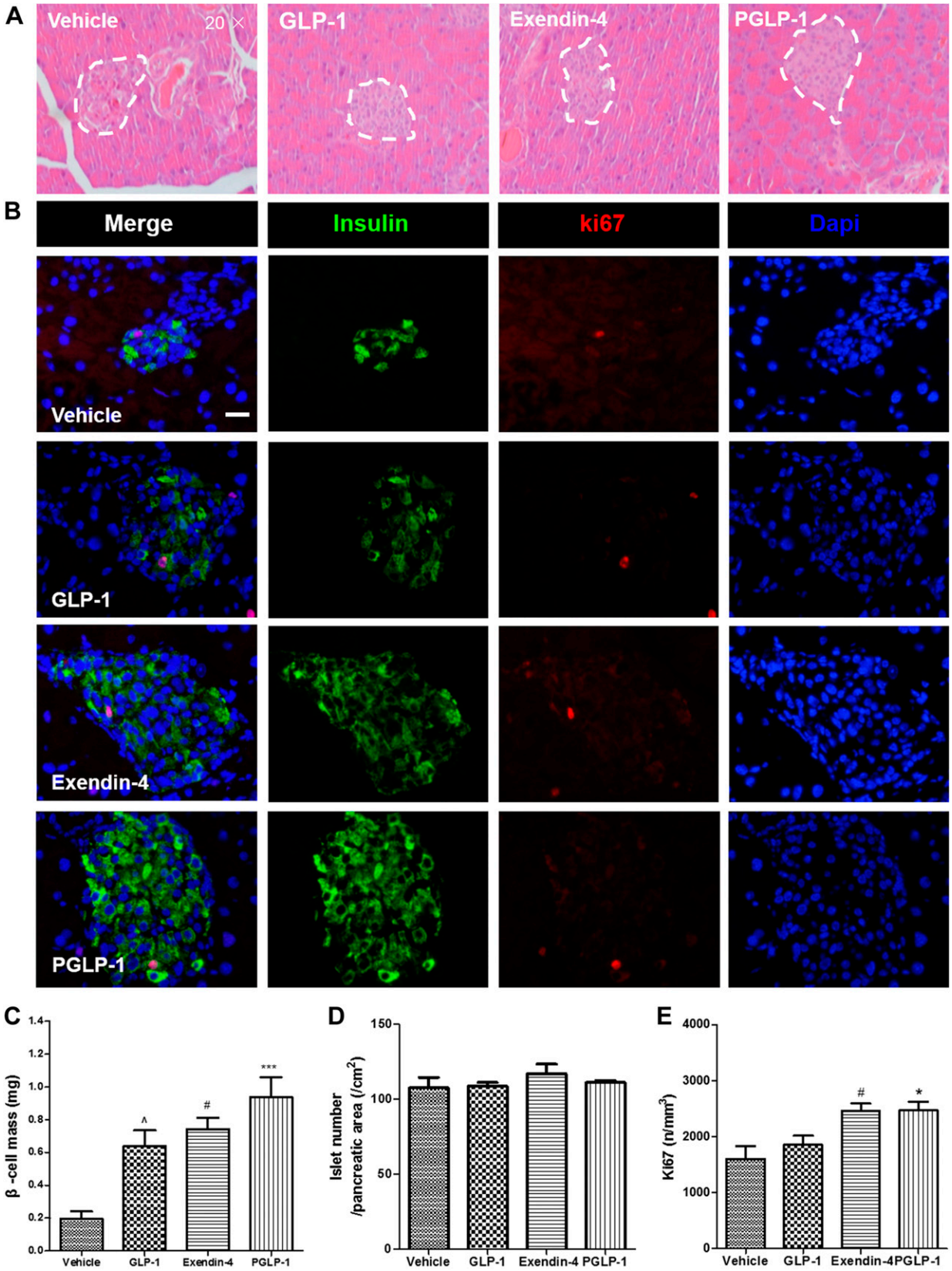


**Figure 6.** Pancreas morphology in STZ-induced hyperglycemic mice. After 5 wk of subcutaneous treatment with placebo, GLP-1 (2 × 30 nmol/kg/d), exendin-4 (2 × 30 nmol/kg/d), or PGLP-1 (2 × 30 nmol/kg/d), mice were humanely killed and pancreata were collected for histologic analyses ($n = 3$ mice per group). *A*) Hematoxylin and eosin staining of pancreas after 5 wk of treatment. *B*) Pancreata were stained with anti-insulin (green) and anti-Ki-67 (red) antibodies and visualized by fluorescence microscopy. Cell nuclei were stained with DAPI (blue). White bar represents 20 μm. *C*—*E*) Stereological estimation of β-cell mass, islet number (number of islet per $cm^2$ pancreas area) (*D*), number of Ki-67-positive β-cell density (number of Ki-67-positive nuclei per $mm^2$ β cells) (*E*). $^*P < 0.05$; $^{**}P < 0.001$, PGLP-1 compared to vehicle group; $^{\wedge}P < 0.05$, GLP-1 compared to vehicle group; $^{\#}P < 0.05$, exendin-4 compared to vehicle group.

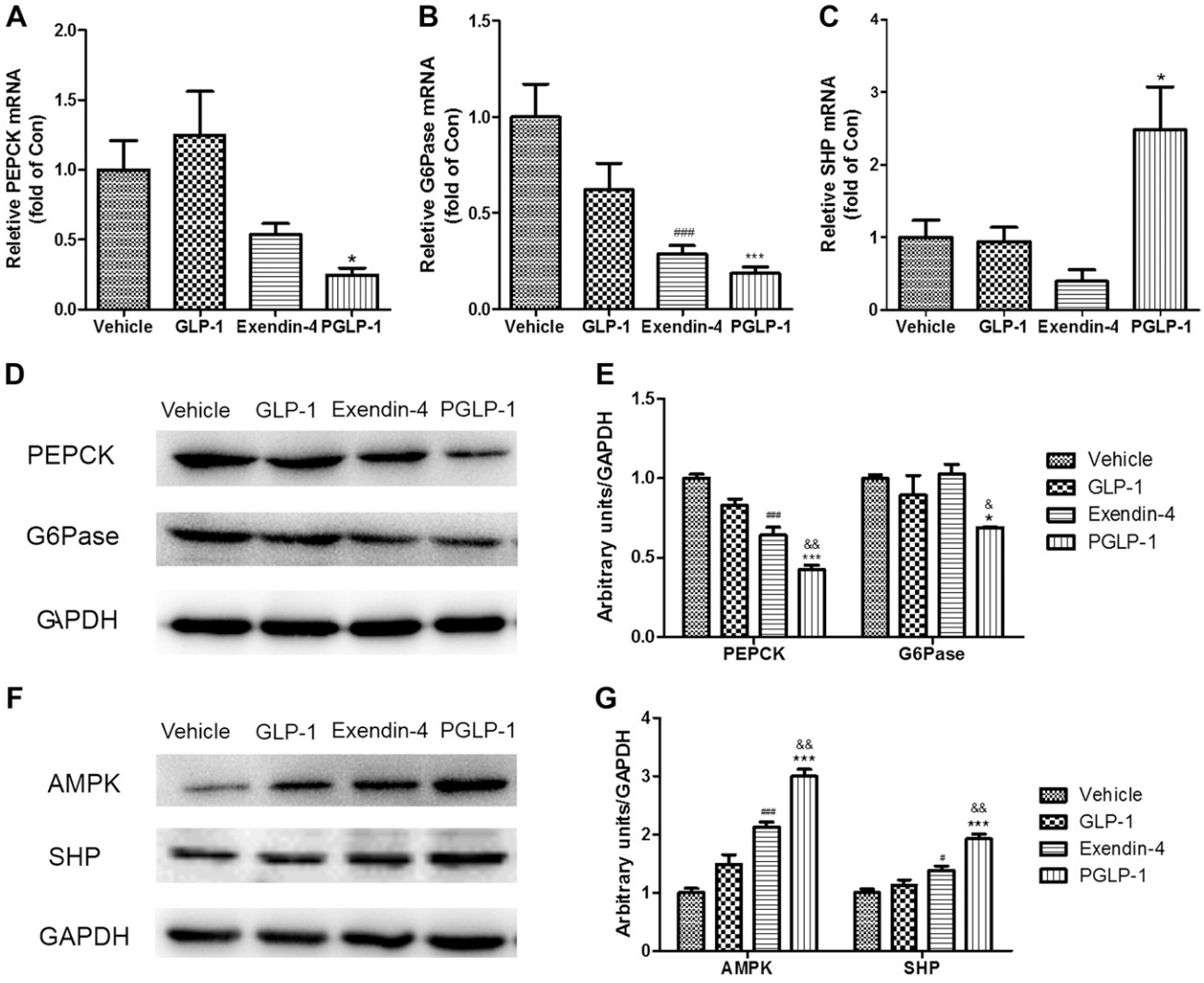


**Figure 7.** PGLP-1 induces changes in expression of genes associated with gluconeogenesis in the liver. After 5 wk of subcutaneous treatment with GLP-1 (2 × 30 nmol/kg/d), exendin-4 (2 × 30 nmol·kg/d), PGLP-1 (2 × 30 nmol/kg/d), or placebo, mice were humanely killed, and livers were collected for assessment of mRNA and protein levels of gluconeogenesis associated genes. *A–C*) Expression of PEPCK (*A*) and G6Pase (*B*) mRNA, and SHP levels (*C*) ($n = 6$ mice per group). *D*) Western blot of PEPCK and G6pase protein in the liver. *E*) Quantification of Western blot ($n = 3$ mice per group). *F*) Western blot of AMPK and SHP protein expression in the liver. *G*) Quantification of Western blot ($n = 3$ mice per group). $^{*}P < 0.05$; $^{***}P < 0.001$, PGLP-1 compared to vehicle group; $^{\#}P < 0.05$; $^{\#\#\#}P < 0.001$ exendin-4 compared to vehicle group; $^{\&}P < 0.001$, $^{\&\&}P < 0.001$ PGLP-1 compared to exendin-4 group.

Previous reports showed that a single administration of rAdGLP-1 improved insulin sensitivity through reducing hepatic gluconeogenesis (28). Consistent with this, PGLP-1 treatment elevated QUICKI and improved glucose and insulin tolerance in STZ-treated mice (Fig. 4*D, H*), suggesting that it can enhance insulin sensitivity. Compared to vehicle, PGLP-1 treatment resulted in lower GTT AUC and ITT AUC than exendin-4, indicating that GLP-1(9-36) amide, a product of PGLP-1 degradation by DPP-IV, also plays an important role besides GLP-1R-mediated effects. This is supported by the report that infusion of GLP-1 (9-36)amide in obese, insulin-resistant human subjects significantly lowered hepatic glucose production (8). Meanwhile, mRNA and protein expression levels of both PEPCK and G6Pase, key regulatory enzymes of gluconeogenesis, were significantly reduced in mice that received PGLP-1 treatment (Fig. 7*A, B, D, E*). This verified that PGLP-1 had an insulinomimetic action, as we hypothesized. However, GLP-1 did not inhibit gluconeogenesis in our study, which conflicts with the report that GLP-1 or GLP-1(9-36)amide can inhibit gluconeogenesis. From the existing reports, we found that the mechanism of drug delivery is different. They all used continuous drug-delivery systems such as rAd-GLP-1 (28), minioosmopump (8), or subcutaneous osmopump (10), but we delivered the drug *via* subcutaneous injection. In addition, GLP-1 has a very short half-life in the circulation. They are rapidly ($t_{1/2} = 1–2$ min) cleaved by the DPP-IV, resulting in the production of the amino-terminally shortened peptides GLP-1(9-36)amide or GLP-1(9-37), with a $t_{1/2}$ of 8 to 10 min (12). Therefore, it is difficult to inhibit the expression of gluconeogenesis genes for a long period of time; the acute action of GLP-1 and GLP-1(9-37) on gluconeogenesis proved this (Fig. 3). Further, to find the mechanism of

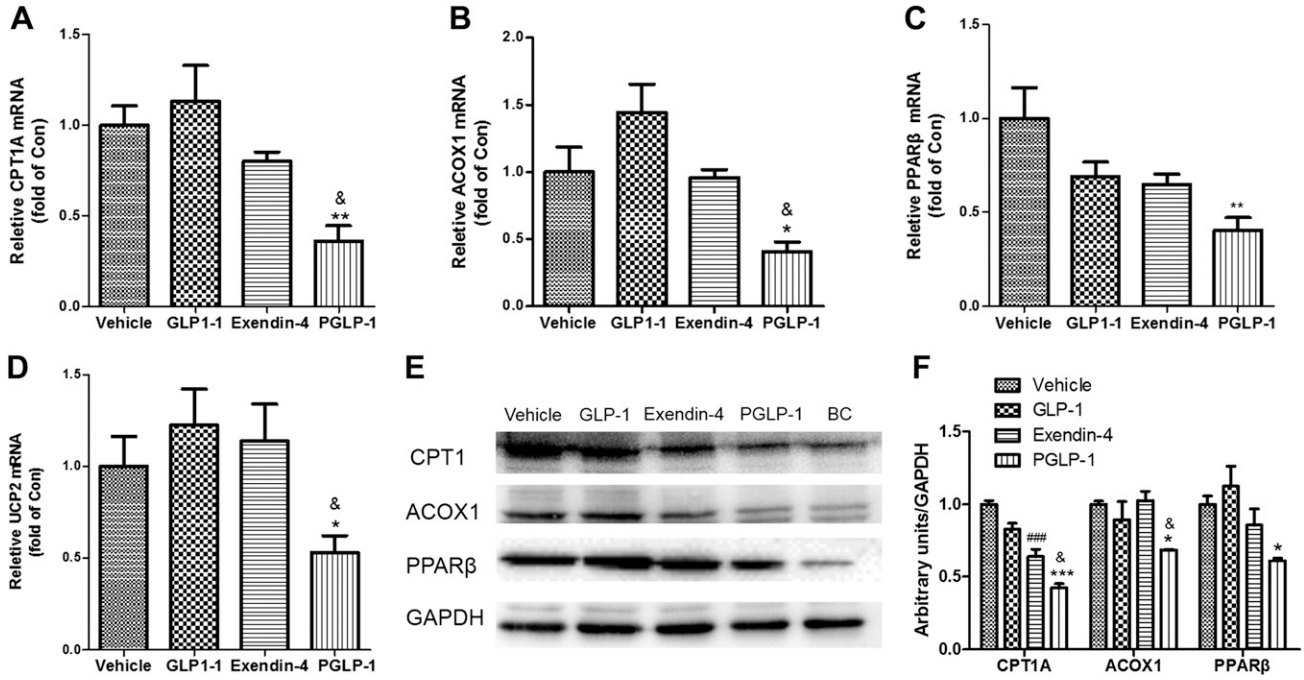


**Figure 8.** Expression of genes associated with β-oxidation in the liver. *A–D*) qPCR measurement of mRNA levels ($n = 6$ mice per group) of CPT1A (*A*), ACOX1 (*B*), PPAR-β/δ (*C*), and UCP-2 (*D*). *E*) Western blots of CPT1A, ACOX1, and PPAR-β/δ protein in the liver. *F*) Quantification of Western blot ($n = 3$ mice per group). BC, blank control. $^{*}P < 0.05$; $^{***}P < 0.001$, PGLP-1 compared to vehicle group; $^{\#}P < 0.05$ exendin-4 compared to vehicle group; $^{\&}P < 0.001$ PGLP-1 compared to exendin-4 group.

inhibiting gluconeogenesis, transcriptional regulators of hepatic gluconeogenesis (29) were analyzed (Supplemental Fig. 4*A–F*), and SHP was a candidate transcriptional regulator (Fig. 7C). The protein levels of SHP and AMPK were significantly increased in mice with PGLP-1 treatment (Fig. 7*F, G*), suggesting a mechanism that PGLP-1 inhibits gluconeogenesis through increasing protein levels of SHP and AMPK. This is consistent with the report that SHP gene expression results in the reduction of hepatic glucose production *via* an AMPK-dependent pathway *in vivo* (30, 31). Given that PGLP-1 treatment increased protein levels of SHP and AMPK more than exendin-4, it is suggested that PGLP-1 suppresses gluconeogenesis through GLP-1R-independent insulinomimetic action (GLP-1(9-36)amide) *via* increasing SHP and AMPK protein levels.

PGLP-1 treatment significantly reduced cumulative energy intake compared to the vehicle group (Fig. 5C), indicating that PGLP-1 could inhibit food intake as a GLP-1R agonist, which is consistent with the report that GLP-1R agonist can inhibit food intake through central regulation (32–34). However, weekly body weight measurements of experimental mice found that STZ-induced hyperglycemic mice with PGLP-1 treatment had significant weight gains (Fig. 5*A, B*). This conflicts with the reports that GLP-1R agonist can inhibit weight gain through inhibition of food intake (33, 34) and that infusion of GLP-1(9-36)amide (10), GLP-1(28-36)amide (35), or GLP-1(32-36)amide (36) can inhibit weight gain through increasing basal energy expenditure. However, PGLP-1 treatment did not increase body weight in normal C57BL/6J mice (data not shown). This indicated that PGLP-1-treated STZ-induced hyperglycemic mice had a higher energy utilization ratio, but it did not induce obesity. Lipid β-oxidation, the main cause of weight loss among STZ-induced hyperglycemic mice (37), was increased in STZ-induced hyperglycemic mice, which is consistent with the report that patients with type 1 diabetes had increased lipid oxidation (23). PGLP-1 treatment significantly inhibited mRNA and protein expression levels of both CPT1A and ACOX1 in the liver (Fig. 8*A, B, E, F*). All these data indicate that PGLP-1 treatment can inhibit body weight loss through decreasing lipid β-oxidation.

Type 1 diabetes is due to β cell destruction, which leads to absolute insulin deficiency (38). When type 1 diabetes becomes clinically manifest, most patients still secrete 20 to 30% insulin compared to nondiabetic individuals, indicating that there is a potentially expandable β-cell mass (39). GLP-1 agonist has beneficial effects on both new onset and long-standing type 1 diabetes mellitus patients, mainly as an adjunctive therapy to insulin in order to improve glycemic control and reduce insulin requirements (40). PGLP-1, a GLP-1 analog, has insulinotropic and insulinomimetic functions. It can increase β-cell mass of islet, improve insulin sensitivity, and inhibit gluconeogenesis, which can improve glycemic control as an adjunctive therapy to insulin in type 1 diabetes mellitus patients. Type 2 diabetes is characterized with dysregulation of hepatic glucose metabolism. During insulin resistant conditions, hepatic glucose production is impaired in part *via* prolonged transcriptional activation of gluconeogenesis (41, 42). PGLP-1, a GLP-1R agonist, stimulates insulin secretion. PGLP-1 simultaneously had insulinomimetic action, which can be used to ameliorate insulin resistance in patients with type 2 diabetes.

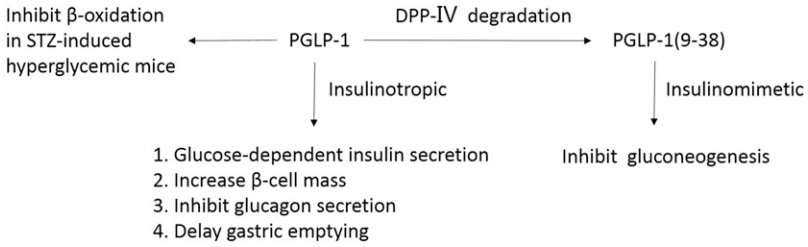


**Figure 9.** Function of PGLP-1 summarized as schematic diagram. PGLP-1, as GLP-1 agonist, has insulinotropic action, including glucose-dependent insulin secretion, inhibition of glucagon section, delay in gastric emptying, and increase in β-cell mass. Simultaneously, PGLP-1 can be degraded into PGLP-1(9-38), which inhibits gluconeogenesis. PGLP-1 inhibits β-oxidation in STZ-induced hyperglycemic mice.

In summary, the findings described here revealed that PGLP-1 might be a novel dual-function (insulinotropic and insulinomimetic) GLP-1R analog (**Fig. 9**). The stability, receptor binding, and glucose-dependent insulin secretion effects of PGLP-1 *in vitro* and *in vivo* verified that PGLP-1 had insulinotropic action as a short GLP-1R agonist. In an STZ-induced hyperglycemic mouse model, PGLP-1 increased β-cell mass of islet, plasma insulin levels, and Ki-67-immunoreactive β-cell mass, which verified that PGLP-1 could work as a short long-acting GLP-1R agonist *in vivo*. Additionally, PGLP-1 improved insulin sensitivity, inhibited gluconeogenesis through increasing expression of AMPK and SHP, and inhibited body weight loss by inhibiting β-oxidation, suggesting that PGLP-1 have insulinomimetic action. Therefore, PGLP-1 may potentially serve as an adjunctive therapy to insulin for the improvement of glycemic control in type 1 diabetes mellitus patients and can be used as a dual-function GLP-1 analog to ameliorate insulin resistance in type 2 diabetes. FJ

## ACKNOWLEDGMENTS

This work was supported, in part, by a project funded by National High Technology Research and Development Program of China (863 Program; 2015AA020314), National Natural Science Foundation of China (81570696 and 31270985), Excellent Youth Foundation of Jiangsu Scientific Committee (BK20140029), Fundamental Research Funds for the Central Universities (Z114037), Priority Academic Program Development of Jiangsu Higher Education Institutions (PAPD), and Top-Notch Academic Programs Project of Jiangsu Higher Education Institutions (PPZY2015A057).

## AUTHOR CONTRIBUTIONS

L. Jin and Y. Zhang designed the experiments; H. Gao performed all the experiments and prepared figures; Q. Zhao, Z. Song, Z. Yang, and Y. Wu helped perform the animal experiments and collected the sample data; H. Gao wrote the article; S. Tang and M. Alahdal reviewed the article; and all authors discussed the research during the experimental period.

## REFERENCES

1. Holst, J. J. (1999) Glucagon-like peptide 1 (GLP-1): an intestinal hormone, signalling nutritional abundance, with an unusual therapeutic potential. *Trends Endocrinol. Metab.* **10**, 229–235
2. Kieffer, T. J., and Habener, J. F. (1999) The glucagon-like peptides. *Endocr. Rev.* **20**, 876–913
3. Hui, H., Zhao, X., and Perfetti, R. (2005) Structure and function studies of glucagon-like peptide-1 (GLP-1): the designing of a novel pharmacological agent for the treatment of diabetes. *Diabetes Metab. Res. Rev.* **21**, 313–331
4. Farilla, L., Hui, H., Bertolotto, C., Kang, E., Bulotta, A., Di Mario, U., and Perfetti, R. (2002) Glucagon-like peptide-1 promotes islet cell growth and inhibits apoptosis in Zucker diabetic rats. *Endocrinology* **143**, 4397–4408
5. Drucker, D. J. (2003) Glucagon-like peptide-1 and the islet beta-cell: augmentation of cell proliferation and inhibition of apoptosis. *Endocrinology* **144**, 5145–5148
6. Abu-Hamdah, R., Rabiee, A., Meneilly, G. S., Shannon, R. P., Andersen, D. K., and Elahi, D. (2009) Clinical review: the extrapancreatic effects of glucagon-like peptide-1 and related peptides. *J. Clin. Endocrinol. Metab.* **94**, 1843–1852
7. Tomas, E., and Habener, J. F. (2010) Insulin-like actions of glucagon-like peptide-1: a dual receptor hypothesis. *Trends Endocrinol. Metab.* **21**, 59–67
8. Elahi, D., Egan, J. M., Shannon, R. P., Meneilly, G. S., Khatri, A., Habener, J. F., and Andersen, D. K. (2008) GLP-1(9-36)amide, cleavage product of GLP-1(7-36)amide, is a glucoregulatory peptide. *Obesity (Silver Spring)* **16**, 1501–1509
9. Tomas, E., Stanojevic, V., and Habener, J. F. (2010) GLP-1(9-36) amide metabolite suppression of glucose production in isolated mouse hepatocytes. *Horm. Metab. Res.* **42**, 657–662
10. Tomas, E., Wood, J. A., Stanojevic, V., and Habener, J. F. (2011) Glucagon-like peptide-1(9-36)amide metabolite inhibits weight gain and attenuates diabetes and hepatic steatosis in diet-induced obese mice. *Diabetes Obes. Metab.* **13**, 26–33
11. Shao, W., Wang, Z., Ip, W., Chiang, Y. T., Xiong, X., Chai, T., Xu, C., Wang, Q., and Jin, T. (2013) GLP-1(28-36) improves β-cell mass and glucose disposal in streptozotocin-induced diabetic mice and activates cAMP/PKA/β-catenin signaling in β-cells *in vitro*. *Am. J. Physiol. Endocrinol. Metab.* **304**, E1263–E1272
12. Deacon, C. F., Nauck, M. A., Toft-Nielsen, M., Pridal, L., Willms, B., and Holst, J. J. (1995) Both subcutaneously and intravenously administered glucagon-like peptide I are rapidly degraded from the NH2-terminus in type II diabetic patients and in healthy subjects. *Diabetes* **44**, 1126–1131
13. Underwood, C. R., Garibay, P., Knudsen, L. B., Hastrup, S., Peters, G. H., Rudolph, R., and Reedtz-Runge, S. (2010) Crystal structure of glucagon-like peptide-1 in complex with the extracellular domain of the glucagon-like peptide-1 receptor. *J. Biol. Chem.* **285**, 723–730
14. Zhang, J., Kulik, H. J., Martinez, T. J., and Klinman, J. P. (2015) Mediation of donor–acceptor distance in an enzymatic methyl transfer reaction. *Proc. Natl. Acad. Sci. USA* **112**, 7954–7959
15. Tiwary, P., Limongelli, V., Salvalaglio, M., and Parrinello, M. (2015) Kinetics of protein–ligand unbinding: predicting pathways, rates, and rate-limiting steps. *Proc. Natl. Acad. Sci. USA* **112**, E386–E391
16. Fitzgerald, L. R., Mannan, I. J., Dytko, G. M., Wu, H. L., and Nambi, P. (1999) Measurement of responses from Gi-, Gs-, or Gq-coupled receptors by a multiple response element/cAMP response element-directed reporter assay. *Anal. Biochem.* **275**, 54–61
17. Like, A. A., and Rossini, A. A. (1976) Streptozotocin-induced pancreatic insulitis: new model of diabetes mellitus. *Science* **193**, 415–417
18. Rossini, A. A., Williams, R. M., Appel, M. C., and Like, A. A. (1978) Sex differences in the multiple-dose streptozotocin model of diabetes. *Endocrinology* **103**, 1518–1520
19. Collombat, P., Mansouri, A., Hecksher-Sorensen, J., Serup, P., Krull, J., Gradwohl, G., and Gruss, P. (2003) Opposing actions of Arx and Pax4 in endocrine pancreas development. *Genes Dev.* **17**, 2591–2603
20. Cai, E. P., Casimir, M., Schroer, S. A., Luk, C. T., Shi, S. Y., Choi, D., Dai, X. Q., Hajmrle, C., Spigelman, A. F., Zhu, D., Gaisano, H. Y., MacDonald, P. E., and Woo, M. (2012) *In vivo* role of focal adhesion

kinase in regulating pancreatic β-cell mass and function through insulin signaling, actin dynamics, and granule trafficking. *Diabetes* **61**, 1708–1718
21. O'Harte, F. P., Mooney, M. H., Lawlor, A., and Flatt, P. R. (2000) *N*-terminally modified glucagon-like peptide-1(7-36)amide exhibits resistance to enzymatic degradation while maintaining its anti-hyperglycaemic activity *in vivo*. *Biochim. Biophys. Acta* **1474**, 13–22
22. Stefan, N., Kantartzis, K., and Häring, H. U. (2008) Causes and metabolic consequences of fatty liver. *Endocr. Rev.* **29**, 939–960
23. Perseghin, G., Lattuada, G., De Cobelli, F., Esposito, A., Costantino, F., Canu, T., Scifo, P., De Taddeo, F., Maffi, P., Secchi, A., Del Maschio, A., and Luzi, L. (2005) Reduced intrahepatic fat content is associated with increased whole-body lipid oxidation in patients with type 1 diabetes. *Diabetologia* **48**, 2615–2621
24. Bojic, L. A., Telford, D. E., Fullerton, M. D., Ford, R. J., Sutherland, B. G., Edwards, J. Y., Sawyez, C. G., Gros, R., Kemp, B. E., Steinberg, G. R., and Huff, M. W. (2014) PPARδ activation attenuates hepatic steatosis in Ldlr$^{-/-}$ mice by enhanced fat oxidation, reduced lipogenesis, and improved insulin sensitivity. *J. Lipid Res.* **55**, 1254–1266
25. Ban, K., Noyan-Ashraf, M. H., Hoefer, J., Bolz, S. S., Drucker, D. J., and Husain, M. (2008) Cardioprotective and vasodilatory actions of glucagon-like peptide 1 receptor are mediated through both glucagon-like peptide 1 receptor-dependent and -independent pathways. *Circulation* **117**, 2340–2350
26. Sonne, D. P., Engstrøm, T., and Treiman, M. (2008) Protective effects of GLP-1 analogues exendin-4 and GLP-1(9-36)amide against ischemia–reperfusion injury in rat heart. *Regul. Pept.* **146**, 243–249
27. Liu, Z., Stanojevic, V., Brindamour, L. J., and Habener, J. F. (2012) GLP1-derived nonapeptide GLP1(28-36)amide protects pancreatic β-cells from glucolipotoxicity. *J. Endocrinol.* **213**, 143–154
28. Lee, Y. S., Shin, S., Shigihara, T., Hahm, E., Liu, M. J., Han, J., Yoon, J. W., and Jun, H. S. (2007) Glucagon-like peptide-1 gene therapy in obese diabetic mice results in long-term cure of diabetes by improving insulin sensitivity and reducing hepatic gluconeogenesis. *Diabetes* **56**, 1671–1679
29. Oh, K. J., Han, H. S., Kim, M. J., and Koo, S. H. (2013) Transcriptional regulators of hepatic gluconeogenesis. *Arch. Pharm. Res.* **36**, 189–200
30. Kim, Y. D., Park, K. G., Lee, Y. S., Park, Y. Y., Kim, D. K., Nedumaran, B., Jang, W. G., Cho, W. J., Ha, J., Lee, I. K., Lee, C. H., and Choi, H. S. (2008) Metformin inhibits hepatic gluconeogenesis through AMP-activated protein kinase-dependent regulation of the orphan nuclear receptor SHP. *Diabetes* **57**, 306–314
31. Lee, J. M., Seo, W. Y., Song, K. H., Chanda, D., Kim, Y. D., Kim, D. K., Lee, M. W., Ryu, D., Kim, Y. H., Noh, J. R., Lee, C. H., Chiang, J. Y., Koo, S. H., and Choi, H. S. (2010) AMPK-dependent repression of hepatic gluconeogenesis *via* disruption of CREB.CRTC2 complex by orphan nuclear receptor small heterodimer partner. *J. Biol. Chem.* **285**, 32182–32191
32. Turton, M. D., O'Shea, D., Gunn, I., Beak, S. A., Edwards, C. M., Meeran, K., Choi, S. J., Taylor, G. M., Heath, M. M., Lambert, P. D., Wilding, J. P., Smith, D. M., Ghatei, M. A., Herbert, J., and Bloom, S. R. (1996) A role for glucagon-like peptide-1 in the central regulation of feeding. *Nature* **379**, 69–72
33. Meeran, K., O'Shea, D., Edwards, C. M., Turton, M. D., Heath, M. M., Gunn, I., Abusnana, S., Rossi, M., Small, C. J., Goldstone, A. P., Taylor, G. M., Sunter, D., Steere, J., Choi, S. J., Ghatei, M. A., and Bloom, S. R. (1999) Repeated intracerebroventricular administration of glucagon-like peptide-1-(7-36)amide or exendin-(9-39) alters body weight in the rat. *Endocrinology* **140**, 244–250 doi:10.1210/endo.140.1.6421
34. Szayna, M., Doyle, M. E., Betkey, J. A., Holloway, H. W., Spencer, R. G., Greig, N. H., and Egan, J. M. (2000) Exendin-4 decelerates food intake, weight gain, and fat deposition in Zucker rats. *Endocrinology* **141**, 1936–1941 doi:10.1210/endo.141.6.7490
35. Ip, W., Shao, W., Chiang, Y. T., and Jin, T. (2013) GLP-1-derived nonapeptide GLP-1(28-36)amide represses hepatic gluconeogenic gene expression and improves pyruvate tolerance in high-fat diet-fed mice. *Am. J. Physiol. Endocrinol. Metab.* **305**, E1348–E1358
36. Tomas, E., Stanojevic, V., McManus, K., Khatri, A., Everill, P., Bachovchin, W. W., and Habener, J. F. (2015) GLP-1(32-36)amide pentapeptide increases basal energy expenditure and inhibits weight gain in obese mice. *Diabetes* **64**, 2409–2419
37. Fruebis, J., Tsao, T. S., Javorschi, S., Ebbets-Reed, D., Erickson, M. R., Yen, F. T., Bihain, B. E., and Lodish, H. F. (2001) Proteolytic cleavage product of 30-kDa adipocyte complement-related protein increases fatty acid oxidation in muscle and causes weight loss in mice. *Proc. Natl. Acad. Sci. USA* **98**, 2005–2010
38. Devendra, D., Liu, E., and Eisenbarth, G. S. (2004) Type 1 diabetes: recent developments. *BMJ* **328**, 750–754
39. Madsbad, S., Krarup, T., Regeur, L., Faber, O. K., and Binder, C. (1980) Insulin secretory reserve in insulin dependent patients at time of diagnosis and the first 180 days of insulin treatment. *Acta Endocrinol.* **95**, 359–363
40. Giorda, C. B., Nada, E., and Tartaglino, B. (2014) Pharmacokinetics, safety, and efficacy of DPP-4 inhibitors and GLP-1 receptor agonists in patients with type 2 diabetes mellitus and renal or hepatic impairment. A systematic review of the literature. *Endocrine* **46**, 406–419 Erratum in: *Endocrine* (2014) 46, 420–422
41. Wan, M., Leavens, K. F., Saleh, D., Easton, R. M., Guertin, D. A., Peterson, T. R., Kaestner, K. H., Sabatini, D. M., and Birnbaum, M. J. (2011) Postprandial hepatic lipid metabolism requires signaling through Akt2 independent of the transcription factors FoxA2, FoxO1, and SREBP1c. *Cell Metab.* **14**, 516–527
42. Taniguchi, C. M., Kondo, T., Sajan, M., Luo, J., Bronson, R., Asano, T., Farese, R., Cantley, L. C., and Kahn, C. R. (2006) Divergent regulation of hepatic glucose and lipid metabolism by phosphoinositide 3-kinase *via* Akt and PKClambda/zeta. *Cell Metab.* **3**, 343–353 Erratum in: *Cell Metab.* (2016) 23, 386.

*Received for publication January 4, 2017.*
*Accepted for publication April 11, 2017.*

# PGLP-1, a novel long-acting dual-function GLP-1 analog, ameliorates streptozotocin-induced hyperglycemia and inhibits body weight loss

Huashan Gao, Qian Zhao, Ziwei Song, et al.

*FASEB J* published online May 1, 2017
Access the most recent version at doi:10.1096/fj.201700002R